Inorganica Chimica Acta 362 (2009) 5175–5182

Contents lists available at ScienceDirect

Inorganica Chimica Acta

journal homepage: www.elsevier.com/locate/ica

Reactivity of phenyldi(2-thienyl)phosphine towards group 7 metal carbonyls: Carbon–phosphorus bond activation

Shishir Ghosh [a], Alok K. Das [a], Noorjahan Begum [b], Daniel T. Haworth [c], Sergey V. Lindeman [c], James F. Gardinier [c], Tasneem A. Siddiquee [d], Dennis W. Bennett [d], Ebbe Nordlander [b,*], Graeme Hogarth [e], Shariff E. Kabir [a,*]

[a] Department of Chemistry, Jahangirnagar University, Savar, Dhaka-1342, Bangladesh
[b] Inorganic Chemistry Research Group, Chemical Physics, Center for Chemistry and Chemical Engineering, Lund University, P. O. Box 124, SE-22100 Lund, Sweden
[c] Department of Chemistry, Marquette University, P. O. Box 1881, Milwaukee, Wisconsin 53201-1881, USA
[d] Department of Chemistry, University of Wisconsin-Milwaukee, P. O. Box 413, Milwaukee, Wisconsin 53211-3029, USA
[e] Department of Chemistry, University College London, 20 Gordon Street, London WC1H 0AJ, UK

ARTICLE INFO

Article history:
Received 7 August 2009
Accepted 4 September 2009
Available online 13 September 2009

Keywords:
Rhenium carbonyl
Manganese carbonyl
Phenyldi(2-thienyl)phosphine
Carbon–phosphorus bond cleavage
X-ray structures

ABSTRACT

Addition of phenyldi(2-thienyl)phosphine ($PPhTh_2$) to $[Re_2(CO)_{10-n}(NCMe)_n]$ ($n = 1, 2$) affords the substitution products $[Re_2(CO)_{10-n}(PhPTh_2)_n]$ (**1**, **2**) together with small amounts of *fac*-$[ClRe(CO)_3(PPhTh_2)_2]$ (**3**) ($n = 2$). Reaction of $[Re_2(CO)_{10}]$ with $PPhTh_2$ in refluxing xylene affords a mixture which includes **2**, $[Re_2(CO)_7(PPhTh_2)(\mu\text{-}PPhTh)(\mu\text{-}H)]$ (**4**), $[Re_2(CO)_7(PPhTh_2)(\mu\text{-}PPhTh)(\mu\text{-}\eta^1,\kappa^1(S)\text{-}C_4H_3S)]$ (**5**) and *mer*-$[HRe(CO)_3(PPhTh_2)_2]$ (**6**). Phosphido-bridged **4** and **5** are formed by the carbon–phosphorus bond cleavage of the coordinated $PPhTh_2$ ligand, the cleaved thienyl group being retained in the latter. Reaction of $[Mn_2(CO)_{10}]$ with $PPhTh_2$ in refluxing toluene affords $[Mn_2(CO)_9(PPhTh_2)]$ (**7**) and the carbon–phosphorus bond cleavage products $[Mn_2(CO)_6(\mu\text{-}PPhTh)(\mu\text{-}\eta^1,\eta^5\text{-}C_4H_3S)]$ (**8**) and $[Mn_2(CO)_5(PPhTh_2)(\mu\text{-}PPhTh)(\mu\text{-}\eta^1,\eta^5\text{-}C_4H_3S)]$ (**9**). Both **8** and **9** contain a bridging thienyl ligand which is bonded to one manganese atom in a η^5-fashion.

1. Introduction

The coordination chemistry of thiophene and its derivatives with transition metal complexes has been extensively explored to understand the nature of the important reactions involved in metal-catalyzed hydrodesulfurization (HDS), a process that removes sulfur from the organosulfur impurities that are commonly found in liquid fuels [1–16]. Numerous examples of thiophene coordination and activation have demonstrated that thiophene and its benzo-derivatives are not useful as ligands for transition metals, even for soft metals that normally bind strongly to sulfur. To overcome this disadvantage, thienyl phosphines have been used to introduce the heterocycle into the metal coordination sphere [17–25].

The reactivity of metal carbonyls of the iron triad with thienyl phosphines such as Ph_2PTh (Th = 2-thienyl) [18–21], $PhPTh_2$ [22], diphenyl(benzothienyl)phosphine [22] and PTh_3 [23,24] is well-documented, and a wealth of intriguing reactivity patterns have been observed. For example, we have recently shown that carbon–sulfur bond scission of a coordinated PTh_3 ligand at a triruthenium center leads to the formation of a μ_3-η^3-1-thia-butadiene ligand [26]. In contrast, the reactivity of group 7 metal carbonyls with thienyl phosphines has not been as extensively studied. Deeming *et al.* have investigated the reactivity of Ph_2PTh with $[Re_2(CO)_{10}]$ and $[Mn_2(CO)_{10}]$ [25] which leads to a number of interesting products (Chart 1). The dirhenium complex $[Re_2(CO)_8(\mu\text{-}\kappa^1,\kappa^1\text{-}Ph_2PC_4H_3S)]$ (**A**) results from the photochemical reaction with $[Re_2(CO)_{10}]$, while in refluxing xylene the isomeric carbon–phosphorus bond cleavage product $[Re_2(CO)_8(\mu\text{-}PPh_2)(\mu\text{-}\eta^1{:}\kappa^1(S)\text{-}C_4H_3S)]$ (**B**) results. With $[Mn_2(CO)_{10}]$ the reaction proceeds differently and in refluxing xylene a mixture of $[Mn_2(CO)_9(Ph_2PTh)]$ (**C**) and $[Mn_2(CO)_6(\mu\text{-}PPh_2)(\mu\text{-}\eta^1{:}\eta^5\text{-}C_4H_3S)]$ (**D**) are obtained. We recently reported the reactivity of PTh_3 with the lightly stabilized dirhenium complexes $[Re_2(CO)_{10-n}(NCMe)_n]$ ($n = 0, 1, 2$) and $[Mn_2(CO)_{10}]$ [27]. With rhenium carbonyls, a series of mono- and dirhenium complexes were obtained (**E**–**M**, Chart 2) while with $[Mn_2(CO)_{10}]$ products **N**–**P** (Chart 2) are similar to those reported with Ph_2PTh. For comparison, we have now investigated the reactivity of $PhPTh_2$ with group 7 metal carbonyls, details of which are reported herein.

* Corresponding authors.
E-mail address: skabir_ju@yahoo.com (S.E. Kabir).

0020-1693/$ - see front matter © 2009 Elsevier B.V. All rights reserved.
doi:10.1016/j.ica.2009.09.021

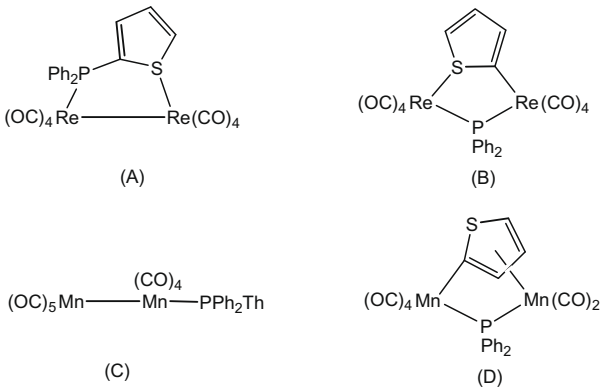

Chart 1.

2. Experimental

$[Re_2(CO)_{10}]$ and $[Mn_2(CO)_{10}]$ were purchased from Strem Chemicals Inc. and used without further purification, and $[Re_2(CO)_9(NCMe)]$ and $[Re_2(CO)_8(NCMe)_2]$ were prepared according to published procedures [28]. Phenyldi(2-thienyl)phosphine ($PPhTh_2$) was purchased from E. Merck and used as received. All reactions were carried out under a nitrogen atmosphere using standard Schlenk techniques. Reagent grade solvents were dried by the standard procedures and were freshly distilled prior to use. Infrared spectra were recorded on a Shimadzu FTIR 8101 spectrophotometer. NMR spectra were recorded on Bruker DPX 400 and Varian Inova 500 instruments. Elemental analyses were performed by Microanalytical Laboratories, University College London. Fast atom bombardment mass spectra were obtained on a JEOL SX-102 spectrometer using 3-nitrobenzyl alcohol as matrix and CsI as calibrant.

2.1. Reaction of $[Re_2(CO)_9(NCMe)]$ with $PPhTh_2$

A CH_2Cl_2 solution (30 mL) of $[Re_2(CO)_9(NCMe)]$ (100 mg, 0.150 mmol) and $PPhTh_2$ (42 mg, 0.153 mmol) was stirred at 25 °C for 90 h. The solvent was removed by rotary evaporation and the residue separated by TLC on silica gel. Elution with hexane/CH_2Cl_2 (7:3, v/v) developed three bands. The first and second bands gave unreacted $[Re_2(CO)_{10}]$ (trace) and $PPhTh_2$ (trace), respectively, while the third band afforded $[Re_2(CO)_9(PPhTh_2)]$ (**1**) (116 mg, 84%) as pale yellow crystals after recrystallization from hexane/CH_2Cl_2 at 4 °C. Spectral data for **1**: *Anal.* Calc. for $C_{23}H_{11}O_9PRe_2S_2$: C, 30.73; H, 1.23. Found: C, 30.96; H, 1.30%. IR (νCO, CH_2Cl_2): 2110 s, 2039 sh, 2009 vs, 1947 s cm^{-1}; ^1H NMR ($CDCl_3$): δ 7.72 (m, 4H), 7.58 (m, 2H), 7.48 (m, 3H), 7.23 (m, 2H); $^{31}P\{^1H\}$ NMR ($CDCl_3$): δ −15.6 (s); MS (FAB): *m/z* 898 (M^+).

2.2. Reaction of $[Re_2(CO)_8(NCMe)_2]$ with $PPhTh_2$

To a CH_2Cl_2 solution (30 mL) of $[Re_2(CO)_8(NCMe)_2]$ (100 mg, 0.147 mmol), $PPhTh_2$ (81 mg, 0.295 mmol) was added and the reaction mixture was stirred at 25 °C for 72 h. The solvent was removed under reduced pressure and the resultant residue was subjected to TLC on silica gel. Elution with hexane/CH_2Cl_2 (7:3, v/v) developed four bands. The first and second bands gave unreacted $[Re_2(CO)_8(NCMe)_2]$ (trace) and $PPhTh_2$ (trace), respectively. The third band afforded $[Re_2(CO)_8(PPhTh_2)_2]$ (**2**) (112 mg, 66%) as yellow crystals while the fourth band gave *fac*-$[ClRe(CO)_3(PPhTh_2)_2]$ (**3**) (27 mg, 21%) after recrystallization from hexane/CH_2Cl_2 at 4 °C. Spectral data for **2**: *Anal.* Calc. for $C_{36}H_{22}O_8P_2Re_2S_4$: C, 37.76; H, 1.94. Found: C, 38.03; H, 1.99%. IR (νCO, CH_2Cl_2): 2016 w, 1990 sh, 1961 vs cm^{-1}; ^1H NMR ($CDCl_3$): δ 7.64 (m, 4H), 7.43 (m, 10H), 7.36 (m, 4H), 7.22 (m, 4H); $^{31}P\{^1H\}$ NMR ($CDCl_3$): δ −11.6 (s); MS (FAB): *m/z* 1146 (M^+). Spectral data for **3**: *Anal.* Calc. for $C_{31}H_{22}ClO_3P_2ReS_4$: C, 43.58; H, 2.60. Found: C, 43.91; H, 2.66%. IR (νCO, CH_2Cl_2): 2039 s, 1960 m, 1907 m cm^{-1}; ^1H NMR ($CDCl_3$): δ 7.56 (m, 4H), 7.49 (m, 4H), 7.33 (m, 7H), 7.23 (m, 3H), 7.03 (m, 4H); $^{31}P\{^1H\}$ NMR ($CDCl_3$): δ −15.1 (s); MS (FAB): *m/z* 854 (M^+).

2.3. Reaction of $[Re_2(CO)_{10}]$ with $PPhTh_2$

A xylene solution (30 mL) of $[Re_2(CO)_{10}]$ (200 mg, 0.307 mmol) and $PPhTh_2$ (168 mg, 0.612 mmol) was heated to reflux for 7 h. The

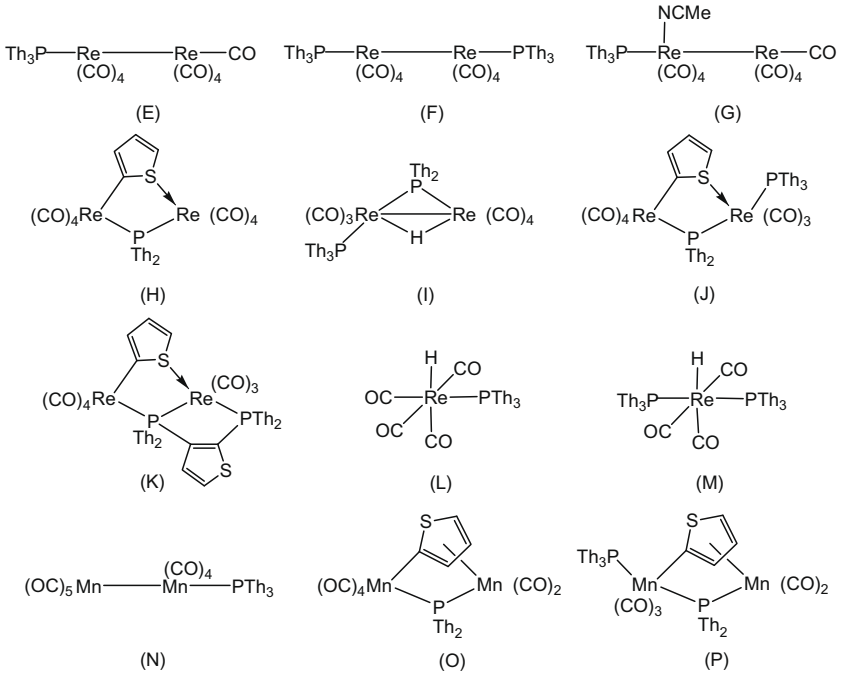

Chart 2.

solvent was removed under reduced pressure and the residue separated by TLC on silica gel. Elution with hexane/CH_2Cl_2 (7:3, v/v) developed nine bands. The first and second bands gave unreacted [$Re_2(CO)_{10}$] (trace) and $PPhTh_2$ (trace), respectively. The fifth to eighth bands afforded the following compounds in order of elution: [$Re_2(CO)_7(PPhTh_2)(\mu$-PPhTh)(μ-H)] (**4**) (96 mg, 30%) as colorless crystals, [$Re_2(CO)_7(PPhTh_2)(\mu$-PPhTh)(μ-η^1,κ^1(S)-C_4H_3S)] (**5**) (64 mg, 19%) as pale yellow crystals, *mer*-[$HRe(CO)_3(PPhTh_2)_2$] (**6**) (43 mg, 17%) as colorless crystals and **2** (47 mg, 13%) after recrystallization from hexane/CH_2Cl_2 at 4 °C. The remaining bands gave minor unidentified products. Spectral data for **4**: *Anal.* Calc. for $C_{31}H_{20}O_7P_2Re_2S_3$: C, 35.97; H, 1.95. Found: C, 36.32; H, 2.03%. IR (νCO, CH_2Cl_2): 2094 m, 2048 m, 1998 vs, 1950 s, 1924 s cm^{-1}; ^1H NMR ($CDCl_3$): δ 7.95 (m, 2H), 7.71 (m, 2H), 7.53–7.23 (m, 14H), 7.00 (m, 1H), −13.85 (dd, J = 16.4, 4.8 Hz, 1H); ^{31}P-{^1H} NMR ($CDCl_3$): δ 24.1 (d, J = 70.4 Hz, 1P), −18.4 (d, J = 70.4 Hz, 1P); MS (FAB): *m/z* 1034 (M^+). Spectral data for **5**: *Anal.* Calc. for $C_{35}H_{22}O_7P_2Re_2S_4$: C, 37.63; H, 1.98. Found: C, 37.98; H, 2.07%. IR (νCO, CH_2Cl_2): 2082 m, 2054 m, 1986 vs, 1974 vs, 1961 vs, 1937 s cm^{-1}; ^1H NMR ($CDCl_3$): δ 7.66 (m, 3H), 7.47 (m, 5H), 7.39 (m, 3H), 7.22 (m, 5H), 7.06 (m, 4H), 6.90 (m, 1H), 6.38 (m, 1H); ^{31}P-{^1H} NMR ($CDCl_3$): δ −21.0 (d, J = 98.0 Hz, 1P), −55.9 (d, J = 98.0 Hz, 1P); MS (FAB): *m/z* 1118 (M^+). Spectral data for **6**: *Anal.* Calc. for $C_{31}H_{23}O_3P_2ReS_4$: C, 45.41; H, 2.83. Found: C, 45.73; H, 2.89%. IR (νCO, CH_2Cl_2): 1938 vs,br, 1917 sh cm^{-1}; ^1H NMR ($CDCl_3$): δ 7.65 (m, 4H), 7.51 (m, 4H), 7.44 (m, 4H), 7.34 (m, 6H), 7.20 (m, 4H), −4.71 (t, J = 20.4 Hz, 1H); ^{31}P-{^1H} NMR ($CDCl_3$): δ −7.9 (s); MS (FAB): *m/z* 820 (M^+).

2.4. Reaction of $[Mn_2(CO)_{10}]$ with $PPhTh_2$

A toluene solution (20 mL) of [$Mn_2(CO)_{10}$] (150 mg, 0.385 mmol) and $PPhTh_2$ (106 mg, 0.386 mmol) was heated to reflux for 4 h. The solvent was removed under reduced pressure and the residue chromatographed by TLC on silica gel. Elution with hexane/CH_2Cl_2 (4:1, v/v) developed five bands. The first band gave unreacted [$Mn_2(CO)_{10}$] (trace). The second, fourth and fifth bands afforded [$Mn_2(CO)_9(PhPTh_2)$] (**7**) (34 mg, 14%) as yellow crystals, [$Mn_2(CO)_6(\mu$-PPhTh)(μ-η^1,η^5-C_4H_3S)] (**8**) (98 mg, 46%) as orange crystals and [$Mn_2(CO)_5(PPhTh_2)(\mu$-PPhTh)(μ-η^1,η^5-C_4H_3S)] (**9**) (92 mg, 30%) as orange crystals after recrystallization from hexane/CH_2Cl_2 at 4 °C. The third band gave a minor unidentified product. Spectral data for **7**: *Anal.* Calc. for $C_{23}H_{11}Mn_2O_9PS_2$: C, 43.41; H, 1.74. Found: C, 43.75; H, 1.80%; IR (ν(CO), CH_2Cl_2): 2091 m, 2064 w, 2012 s, 1993 vs, 1972 m, 1958 m, 1938 cm^{-1}; ^1H NMR ($CDCl_3$): δ 7.56 (m, 2H), 7.20 (m, 2H), 7.01 (m, 7H); ^{31}P-{^1H} NMR ($CDCl_3$): δ 58.6 (s); MS (FAB): *m/z* 636 (M^+). Spectral data for **8**: *Anal.* Calc. for $C_{20}H_{11}Mn_2O_6PS_2$: C, 43.49; H, 2.01. Found: C, 43.81; H, 2.07%; IR (ν(CO), CH_2Cl_2): 2068 s, 1991 s, 1975 vs, 1961 vs, 1909 s cm^{-1}; ^1H NMR ($CDCl_3$): δ 7.83 (m, 2H), 7.63 (m, 2H), 7.48 (m, 3H), 7.34 (m, 7H), 7.08 (s, br, 2H), 6.21 (s, br, 1H), 6.14 (s, br, 1H), 5.81 (m, 2H), 5.76 (s, br, 1H), 5.73 (s, br, 1H); ^{31}P-{^1H} NMR ($CDCl_3$): δ −33.8 (s, 1P), −43.2 (s, 1P); MS (FAB): *m/z* 552 (M^+). Spectral data for **9**: *Anal.* Calc. for $C_{33}H_{22}Mn_2O_5P_2S_4$: C, 49.63; H, 2.78. Found: C, 49.96; H, 2.85%; IR (ν(CO), CH_2Cl_2): 2018 w, 1956 vs, 1931 vs, 1911 s, 1900 s cm^{-1}; ^1H NMR ($CDCl_3$): δ 7.88 (m, 2H), 7.76 (m, 2H), 7.54 (m, 4H), 7.50–7.27 (m, 24H), 7.12 (m, 4H), 7.04 (m, 2H), 5.85 (s, br, 1H), 5.75 (s, br, 1H), 5.66 (m, 2H), 5.55 (m, 1H), 5.52 (m, 1H); ^{31}P-{^1H} NMR ($CDCl_3$): δ 51.4 (s, 2P), −12.9 (s, 1P), −21.6 (s, 1P); MS (FAB): *m/z* 798 (M^+).

2.5. Conversion of **8**–**9**

A toluene solution (15 mL) of **8** (50 mg, 0.091 mmol) was heated to reflux for 3 h. Workup afforded unreacted **8** (trace) and **9** (39 mg, 54%).

2.6. X-ray crystallographic studies

Single crystals of compounds **3**, **4**, **6**, **8** and **9** suitable for X-ray diffraction were obtained by recrystallization from hexane/CH_2Cl_2 at room temperature and mounted on Nylon fibers with a mineral oil, and diffraction data were collected at 100(2) K on a Bruker AXS SMART diffractometer equipped with an APEX CCD detector using graphite-monochromated Cu Kα radiation (λ = 1.54178 Å). Integration of intensities and data reduction was performed using the SAINT program [29]. Numerical (based on the real shape of the crystals) absorption correction was applied in all cases followed by the multi-scan SADABS procedure [30]. The structures were solved by direct methods [31] and refined by full-matrix least-squares on F^2 [32]. All non-hydrogen atoms were refined anisotropically. Pertinent crystallographic data and structure refinement parameters are summarized in Table 1.

3. Results and discussion

3.1. Reactions of $[Re_2(CO)_{10-n}(NCMe)_n]$ (**n** = 1,2) with $PhPTh_2$: substitution products

Treatment of [$Re_2(CO)_9(NCMe)$] with $PPhTh_2$ at 25 °C afforded the substitution product [$Re_2(CO)_9(PPhTh_2)$] (**1**) (84%), while [$Re_2(CO)_8(NCMe)_2$] similarly gave [$Re_2(CO)_8(PPhTh_2)_2$] (**2**) (66%). Both are readily characterized by comparison of spectroscopic data with related [$Re_2(CO)_{10-n}(L)_n$] complexes (n = 1,2: L = PPh_3, PMe_3, PTh_3, PFu_3) [27,28b,33]. In the ^{31}P-{^1H} NMR spectra, both display only a singlet, at δ −15.6 for **1** and −11.6 for **2**, suggesting that the phosphines occupy axial sites in both compounds [27,33] (Scheme 1).

An additional product was isolated from the reaction of the bis(acetonitrile) starting material, and it was shown to be *fac*-[$ClRe(CO)_3(PPhTh_2)_2$] (**3**) (21%) as confirmed by an X-ray crystallographic study. An ORTEP diagram of the molecular structure of **3** is depicted in Fig. 1. and selected bond distances and angles are listed in the caption. The basic structure of **3** is very similar to that of the recently reported *fac*-[$ClRe(CO)_3(\kappa^2$-dppn)] (dppn = 1,8-bis(diphenylphosphino)naphthalene) [34]. The molecule consists of a single rhenium atom with three carbonyl groups arranged in a *facial* arrangement, two $PPhTh_2$ ligands and a chloride ligand. The overall coordination geometry is a distorted octahedron which is evident from the expansion of P–Re–P angle to 103.06(2)°, presumably a result of adverse steric interactions. The *trans* angles about rhenium range from 168.6(3)° to 176.6(4)° which are comparable to the corresponding angles in *fac*-[$Re(CO)_3(\kappa^1$(P),η^1-$PPh_2C_{10}H_6$)(PPh_2H)] which range from 168.62(9)° to 172.48(9)° [34]. The rhenium–phosphorus distances of 2.494(2) Å and 2.520(2) Å are similar to those in reported in the literature for related complexes [25,27,33,34]. The source of the chloride ligand was not identified; we speculate that it comes from the chlorinated solvent during chromatographic separation or recrystallization. The rhenium–chlorine bond distance of 2.514(4) Å is within the expected range [34]. Spectroscopic data for **3** are consistent with the solid-state structure. The ^1H NMR spectrum displays only aromatic protons, while the ^{31}P-{^1H} NMR spectrum consists of a singlet at δ −15.1. The FAB mass spectrum shows a parent molecular ion at *m/z* 854.

3.2. Thermal reaction of $[Re_2(CO)_{10}]$ and $PhPTh_2$: selective carbon–phosphorus bond scission

Since at ambient temperature only simple substitution products were observed, we investigated the elevated temperature reaction between [$Re_2(CO)_{10}$] and $PPhTh_2$. In refluxing xylene, both **2** (13%)

Table 1
Crystallographic data for compounds **3**, **4**, **6**, **8** and **9**.

Compound	**3**	**4**	**6**	**8**	**9**
Empirical formula	$C_{31}H_{22}ClO_{3.30}P_2ReS_4$	$C_{31}H_{20}O_7P_2Re_2S_3$	$C_{31}H_{23}O_3P_2ReS_4$	$C_{20}H_{11}Mn_2O_6PS_2$	$C_{33}H_{22}Mn_2O_5P_2S_4$
Formula weight (Å)	859.04	1034.99	819.87	552.26	798.57
Temperature (K)	100(2)	100(2)	100(2)	100(2)	100(2)
Wavelength (Å)	1.54178	1.54178	1.54178	1.54178	1.54178
Crystal system	monoclinic	monoclinic	monoclinic	monoclinic	monoclinic
Space group	*Pn*	$P2_1/n$	$C2/c$	$P2_1/n$	$P2_1/c$
Unit cell dimensions					
a (Å)	9.5825(3)	13.2604(2)	16.8770(5)	15.9950(4)	18.2626(5)
b (Å)	8.8810(3)	11.4601(2)	9.6013(3)	9.0185(2)	11.8253(3)
c (Å)	18.6992(5)	22.4574(4)	19.6843(6)	16.0234(4)	17.0579(5)
a (°)	90	90	90	90	90
b (°)	90.5420(10)	104.2630(10)	103.4030(10)	113.2600(10)	117.307(2)
c (°)	90	90	90	90	90
Volume (Å^3)	1591.27(8)	3307.55(10)	3102.79(16)	2123.53(9)	3273.31(16)
Z	2	4	4	4	4
Density (calculated) (Mg m^{-3})	1.793	2.078	1.755	1.727	1.62
Absorption coefficient (mm^{-1})	11.925	17.173	11.416	12.554	9.94
F(0 0 0)	841	1960	1608	1104	1616
Crystal size (mm)	0.37 × 0.29 × 0.04	0.42 × 0.22 × 0.10	0.23 × 0.15 × 0.10	0.49 × 0.30 × 0.20	0.40 × 0.30 × 0.20
θ range for data collection (°)	4.73–66.91	4.06–68.02	4.62–67.17	3.31–61.48	2.72–61.32
Index ranges	$-11 \leqslant h \leqslant 10$, $-0 \leqslant k \leqslant 10$, $-22 \leqslant l \leqslant 21$	$-15 \leqslant h \leqslant 15$, $0 \leqslant k \leqslant 13$, $0 \leqslant l \leqslant 26$	$-19 \leqslant h \leqslant 19$, $0 \leqslant k \leqslant 11$, $0 \leqslant l \leqslant 22$	$-18 \leqslant h \leqslant 16$, $0 \leqslant k \leqslant 10$, $0 \leqslant l \leqslant 18$	$-20 \leqslant h \leqslant 18$, $0 \leqslant k \leqslant 13$, $0 \leqslant l \leqslant 19$
Reflections collected	13161	27360	12995	17449	26627
Independent reflections (R_{int})	5170 [R_{int} = 0.0214]	5915 [R_{int} = 0.0252]	2692 [R_{int} = 0.0177]	3225 [R_{int} = 0.0272]	4968 [R_{int} = 0.0391]
Refinement method	full-matrix least-squares on F^2	full-matrix least-squares on F^2	full-matrix least-squares on F^2	full-matrix least-squares on F^2	full-matrix least-squares on F^2
Data/restraints/ parameters	5170/301/366	5915/182/389	2692/30/237	3225/30/226	4968/282/382
Goodness-of-fit (GOF) on F^2	1.003	1.039	1.11	1.203	1.019
Final *R* indices [$I > 2s(I)$]	R_1 = 0.0185, wR_2 = 0.0457	R_1 = 0.0307, wR_2 = 0.0736	R_1 = 0.0155, wR_2 = 0.0391	R_1 = 0.0405, wR_2 = 0.1003	R_1 = 0.0621, wR_2 = 0.1474
R indices (all data)	R_1 = 0.0189, wR_2 = 0.0459	R_1 = 0.0323, wR_2 = 0.0745	R_1 = 0.0156, wR_2 = 0.0392	R_1 = 0.0414, wR_2 = 0.1008	R_1 = 0.0666, wR_2 = 0.1502
Largest diff. peak and hole (e Å^{-3})	0.622 and −0.410	1.351 and −0.989	0.503 and −0.330	2.184 and −0.888	0.830 and −0.937

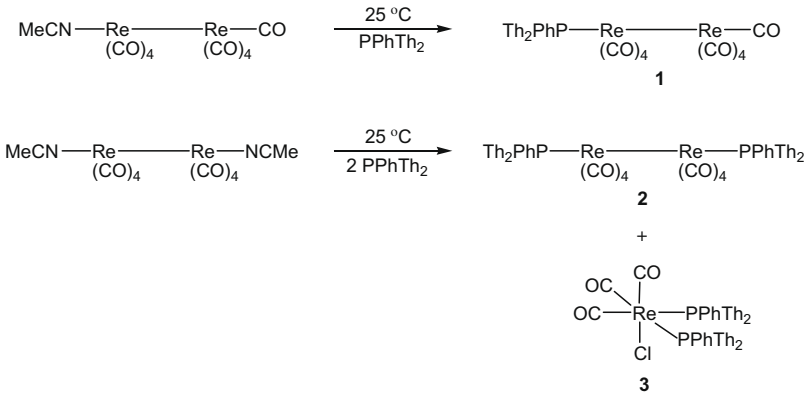

Scheme 1.

and three new compounds were formed, viz. $[Re_2(CO)_7(PPhTh_2)(\mu\text{-}PPhTh)(\mu\text{-}H)]$ (**4**) (30%), $[Re_2(CO)_7(PPhTh_2)(\mu\text{-}PPhTh)(\mu\text{-}\eta^1, \kappa^1(S)\text{-}C_4H_3S)]$ (**5**) (19%) and *mer*-$[HRe(CO)_3(PPhTh_2)_2]$ (**6**) (17%) (Scheme 2).

All three new compounds have been characterized by elemental analysis and spectroscopic data, as well as single crystal X-ray diffraction studies for **4** and **6**. An ORTEP diagram of the molecular structure of **4** is depicted in Fig. 2. The disordered crystal contains two enantiomers, each containing a dirhenium core with seven terminal carbonyl groups, a bridging phenyl(2-thienyl)phosphido group, an intact $PPhTh_2$ ligand and a bridging hydride. The hydride ligand was located and refined in the structural analysis [Re(1)–H(1H) 1.90(7) Å and Re(2)–H(1H) 1.92(7) Å]. The phenyl(2-thienyl)phosphido ligand bridges the rhenium–rhenium vector somewhat asymmetrically [Re(1)–P(1) 2.3923(13) Å and Re(2)–P(1) 2.4336(13) Å] and the $PPhTh_2$ ligand occupies an equatorial site

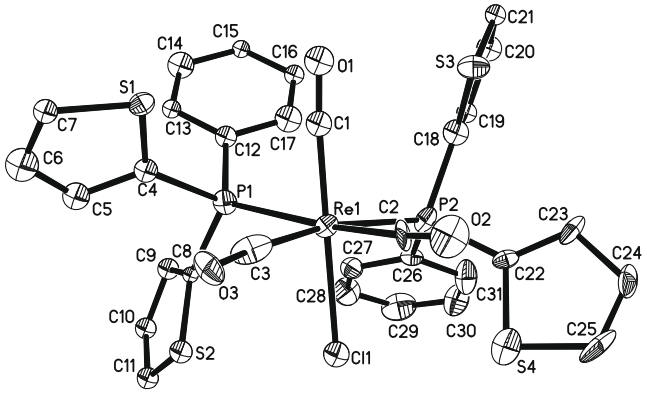

Fig. 1. Molecular structure of *fac*-[ClRe(CO)$_3$(PPhTh$_2$)$_2$] (**3**) showing 50% probability thermal ellipsoids. Ring hydrogens are omitted for clarity. Selected bond lengths (Å) and angles (°): Re(1)–P(1) 2.494(2), Re(1)–P(2) 2.520(2), Re(1)–Cl(1) 2.514(4), Re(1)–C(1) 1.917(9), Re(1)–C(2) 1.961(7), Re(1)–C(3) 1.961(10), C(1)–Re(1)–C(2) 89.6(4), C(1)–Re(1)–C(3) 91.2(5), C(2)–Re(1)–C(3) 86.64(12), C(1)–Re(1)–P(1) 82.8(4), C(1)–Re(1)–P(2) 97.5(4), C(2)–Re(1)–P(1) 168.8(2), C(3)–Re(1)–P(1) 85.3(3), C(2)–Re(1)–P(2) 86.0(3), C(3)–Re(1)–P(2) 168.6(3), C(1)–Re(1)–Cl(1) 176.6(4), C(2)–Re(1)–Cl(1) 92.7(2), C(3)–Re(1)–Cl(1) 91.4(2), P(1)–Re(1)–Cl(1) 95.22(8), Cl(1)–Re(1)–P(2) 80.22(9), P(1)–Re(1)–P(2) 103.06(2), O(1)–C(1)–Re(1) 174.9(12), O(2)–C(2)–Re(1) 175.1(7), O(3)–C(3)–Re(1) 174.3(8).

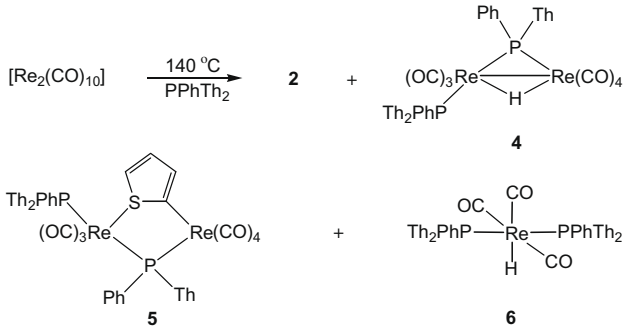

Scheme 2.

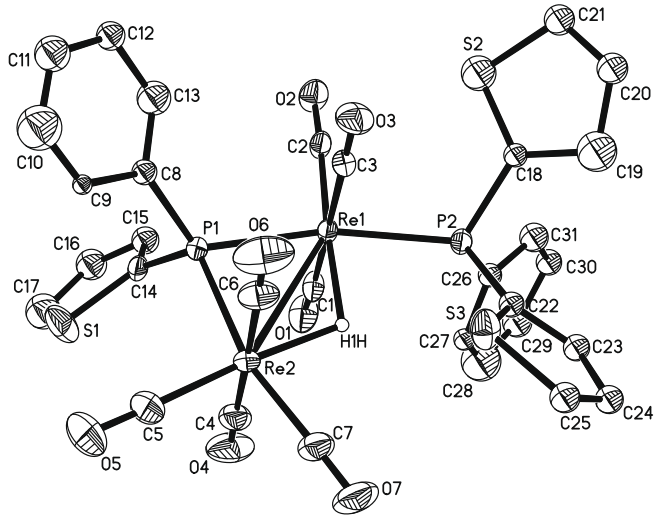

Fig. 2. Molecular structure of [Re$_2$(CO)$_7$(PPhTh$_2$)(μ-PPhTh)(μ-H)] (**4**) showing 50% probability thermal ellipsoids. Ring hydrogens are omitted for clarity. Selected bond lengths (Å) and angles (°): Re(1)–Re(2) 3.1497(3), Re(1)–P(1) 2.3923(13), Re(1)–P(2) 2.4162(12), Re(2)–P(1) 2.4336(13), Re(1)–H(1H) 1.90(7), Re(2)–H(1H) 1.92(7), C(2)–Re(1)–C(3) 88.8(2), C(2)–Re(1)–C(1) 87.6(2), C(3)–Re(1)–C(1) 176.4(2), C(2)–Re(1)–P(1) 100.08(15), C(3)–Re(1)–P(1) 91.09(15), C(1)–re(1)–P(1) 90.17(16), C(2)–Re(1)–P(2) 96.31(15), C(3)–Re(1)–P(2) 86.56(15), C(1)–Re(1)–P(2) 93.19(15), P(1)–Re(1)–P(2) 163.39(4), P(1)–Re(1)–Re(2) 49.83(3), P(1)–Re(2)–Re(1) 48.69(3), P(1)–Re(1)–H(1H) 84(2), P(1)–Re(2)–H(1H) 83(2), P(2)–Re(1)–H(1H) 80(2), C(7)–Re(2)–H(1H) 83(2), C(2)–Re(1)–H(1H) 174(2), C(5)–Re(2)–H(1H) 176(2), Re(2)–Re(1)–H(1H) 35(2), Re(1)–Re(2)–H(1H) 34(2), C(7)–Re(2)–P(1) 165.63(19), C(6)–Re(2)–P(1) 89.35(17), C(5)–Re(2)–P(1) 100.5(2), C(5)–Re(2)–C(7) 93.8(3), C(5)–Re(2)–C(6) 89.1(3), C(5)–Re(2)–C(4) 91.5(3), C(6)–Re(2)–C(4) 178.1(2), Re(1)–P(1)–Re(2) 81.48(4), C(14)–P(1)–C(8) 104.6(5).

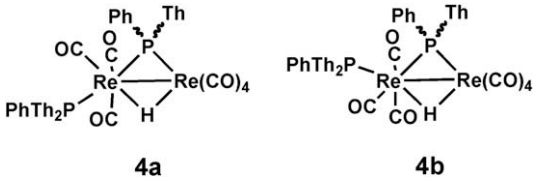

Chart 3.

and lies *trans* to the phosphido-bridge [P(1)–Re(2)–P(2) 163.39(4)°]. The Re–Re bond length of 3.1497(3) Å is similar to that found in [Re$_2$(CO)$_7$(PTh$_3$)(μ-PTh$_2$)(μ-H)] (**I**) [3.1555(2) Å] (Chart 2) and the IR spectrum also closely resembles that of **I** [33]. In the solid-state structure the thienyl and phenyl groups are clearly distinguished, but occupy chemically inequivalent sites. The ^{31}P-{^{1}H} NMR spectrum clearly indicates the existence of two isomeric forms in solution in an approximate 10:1 ratio. The major isomer (probably that seen in the solid-state (**4a**, Chart 3), with the phosphine in relative *trans* position to the thienyl substituent of the bridging phosphido moiety), consists of two doublets at δ 24.1 and −18.4 (J_{PP} = 70.4 Hz), while there is also a second set of doublets at δ −8.4 and −17.9 (J_{PP} = 76.4 Hz) attributed to the minor isomer (Chart 3). Both sets of signals are sharp and we have no evidence for the interconversion of the two. Apparently, this isomer has the phosphine in the *cis* position relative to the bridging phosphido moiety. Steric crowding of the P–P groupings gives energies of 861 vs. 843 kJ/mol for the *trans* isomer. The crystal of **4a** contains two enantiomers in a 50/50 ratio (Chart 3).

All attempts to obtain single crystals of **5** suitable for X-ray diffraction analysis were unsuccessful and characterization has therefore been made on the basis of analytical and spectroscopic data. The IR spectrum is very similar to that of [Re$_2$(CO)$_7$(PTh$_3$)(μ-PTh$_2$)(μ-η^1,κ^1(S)-C$_4$H$_3$S)] (**J**) (Chart 2), indicating that the two are isostructural. The ^{1}H NMR spectrum shows seven multiplets in the aromatic region with the relative intensity of 3:5:3:5:4:1:1 which are assigned to the phenyl and thienyl ring protons. In addition, the multiplet at δ 6.38 (integrating to 1H) is indicative of an orthometallated thienyl or phenyl ring. The ^{31}P-{^{1}H} NMR spectrum again indicates the presence of two isomers in solution in an approximate 20:1 ratio. The major isomer shows doublets at δ −21.0 and −55.9 (J_{PP} = 98.0 Hz), while the minor exhibits doublets at δ −19.1 (J = 116.4 Hz) and −53.7 (J_{PP} = 116.4 Hz); these isomers are probably isomers (diastereomers) of the same kind observed for **4**, but may also be diastereomers formed by the combination of the stereogenic centers at the sulfur and the bridging phosphido moiety (or combinations of these types of isomers). The FAB mass spectrum shows a molecular ion at *m/z* 1118 and fragmentation ions due to sequential loss of seven carbonyl groups. Elemental analysis (cf. Section 2.3) was also consistent with the empirical formula.

An ORTEP diagram of the molecular structure of **6** is shown in Fig. 3. and selected bond distances and angles are listed in the caption. The molecule has two crystallographic planes of symmetry and contains a single rhenium atom ligated by three carbonyls, two phosphines and a hydride. The latter was located and refined in the structural analysis [Re(1)–H(1H) 1.73(6) Å]. The PPhTh$_2$ ligands lie *trans* [P(1)–Re(1)–P(1)#1 166.47(3)°] presumably to minimize steric hindrance. While in **3** the carbonyls are arranged in a *facial* fashion in **6** they adopt a *meridional* arrangement. The

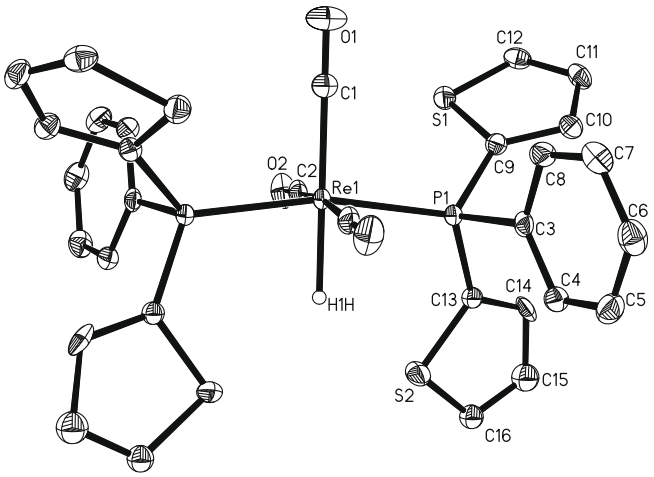

Fig. 3. Molecular structure of *mer*-[HRe(CO)$_3$(PPhTh$_2$)$_2$] (**6**) showing 50% probability thermal ellipsoids. Ring hydrogens are omitted for clarity. Selected bond lengths (Å) and angles (°): Re(1)–P(1) 2.3849(5), Re(1)–P(1)#1 2.3849(5), Re(1)–H(1H) 1.73(6), Re(1)–C(1) 1.957(3), Re(1)–C(2) 1.986(2), Re(1)–C(2)#1 1.986(2), C(1)–Re(1)–C(2) 93.41(6), C(1)–Re(1)–C(2)#1 93.41(6), C(2)–Re(1)–C(2)#1 173.18(12), C(1)–Re(1)–P(1) 96.767(13), C(1)–Re(1)–P(1)#1 96.766(12), C(2)–Re(1)–P(1) 91.11(6), C(2)#1–Re(1)–P(1) 88.09(6), C(2)–Re(1)–P(1)#1 88.09(6), C(2)#1–Re(1)–P(1)#1 91.10(6), C(1)–Re(1)–H(1H) 180.00(2), C(2)–Re(1)–H(1H) 86.59(6), C(2)#1–Re(1)–H(1H) 86.59(6), P(1)–Re(1)–H(1H) 83.233(13), P(1)#1–Re(1)–H(1H) 83.23(2), P(1)–Re(1)–P(1)#1 166.47(3), O(1)–C(1)–Re(1) 180.000(1), O(2)–C(2)–Re(1) 177.24(19).

structure is very similar to that of *mer*-[HRe(CO)$_3$(PPh$_3$)$_2$] [35] and *mer*-[HRe(CO)$_3$(PTh$_3$)$_2$] [27]. Spectroscopic data suggests that the solid-state structure persists in solution. The ^{1}H NMR spectrum shows a triplet at δ −4.71 (J_{PH} = 20.4 Hz) due to the hydride, while the ^{31}P{^{1}H} NMR spectrum contains only a singlet at δ −7.9 due to two equivalent phosphorus atoms.

3.3. Reaction of [Mn$_2$(CO)$_{10}$] with PPhTh$_2$: carbon–phosphorus bonds cleavage

Since the reactivity of [Mn$_2$(CO)$_{10}$] with PPh$_2$Th [25] closely parallels that established previously for PTh$_3$ [27], we also conducted for comparison the reaction of [Mn$_2$(CO)$_{10}$] with PPhTh$_2$. In refluxing toluene three new complexes were formed, namely [Mn$_2$(CO)$_9$(PPhTh$_2$)] (**7**) (14%), [Mn$_2$(CO)$_6$(μ-PPhTh)(μ-η^1,η^5-C$_4$H$_3$S)] (**8**) (46%) and [Mn$_2$(CO)$_5$(PPhTh$_2$)(μ-PPhTh)(μ-η^1,η^5-C$_4$H$_3$S)] (**9**) (30%) (Scheme 3). In a separate experiment we also showed that **8** is converted into **9** when treated with PPhTh$_2$ under the same conditions. These results are similar to those observed for PTh$_3$ [27]. The structure of **7** is easily assigned on the basis of spectroscopic data - the IR spectrum being very similar to other substituted [Mn(CO)$_9$L] compounds (L = PTh$_3$, PPhTh$_2$, diphenyl(1-naphthyl)phosphine) [25,27,34]. The ^{31}P-{^{1}H} NMR spectrum displays only a singlet at δ 58.6 and the FAB mass spectrum exhibits a parent molecular ion at *m/z* 636 consistent with the proposed structure.

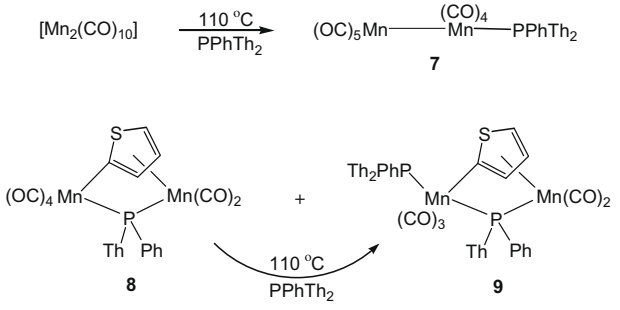

Scheme 3.

An ORTEP diagram of the molecular structure of **8** is shown in Fig. 4. and selected bond distances and angles are listed in the caption. The molecule consists of a dinuclear framework of two manganese atoms coordinated by six carbonyl groups, a phenylthienyl phosphido bridge and a thienyl bridge. The structure is very similar to the PPh$_2$Th and PTh$_3$ analogs [Mn$_2$(CO)$_6$(μ-PPh$_2$)(μ-η^1,η^5-C$_4$H$_3$S)] (**D**) (Chart 1) and [Mn$_2$(CO)$_6$(μ-PTh$_2$)(μ-η^1,η^5-C$_4$H$_3$S)] (**O**) (Chart 2). The phosphido ligand bridges the dimanganese center [Mn...Mn 3.510(1) Å] quite asymmetrically [Mn(1)–P(1) 2.3711(11) Å and Mn(2)–P(1) 2.2848(11) Å]. The bridging thienyl ligand is bound to one manganese atom by a simple σ-bond [Mn(1)–C(10) 2.079(4) Å], but it binds to the second in an η^5-fashion with manganese–carbon bond distances ranging between 2.129(4) and 2.195(4) Å. This is very similar to the situation found in **D** and **O** and we therefore conclude that it acts as an overall 7-electron donor ligand. As a result, Mn(1) has an octahedral coordination sphere, while Mn(2) possesses a half-sandwich geometry. Both ^{1}H NMR and ^{31}P-{^{1}H} NMR spectra suggest that it exists in two isomeric (diastereomeric) forms in solution. For example, the latter spectrum shows two equal intensity singlets at δ −33.8 and −43.2. As discussed above, it is likely that the diastereomers are formed by the combination of the stereogenic centers at the sulfur and the bridging phosphido moiety (or combinations of these types of isomers). The π-complexation of a thienyl ring is also indicated by the upfield resonances in the ^{1}H NMR spectrum at δ 6.21, 6.14, 5.81, 5.76 and 5.73 in a 1:1:2:1:1 ratio. The FAB mass spectrum exhibits a parent molecular ion at *m/z* 552 plus other ions due to stepwise loss of six carbonyl ligands, which is in accord with the solid-state structue.

An ORTEP diagram of the molecular structure of **9** is shown in Fig. 5. and selected bond distances and angles are listed in the cap-

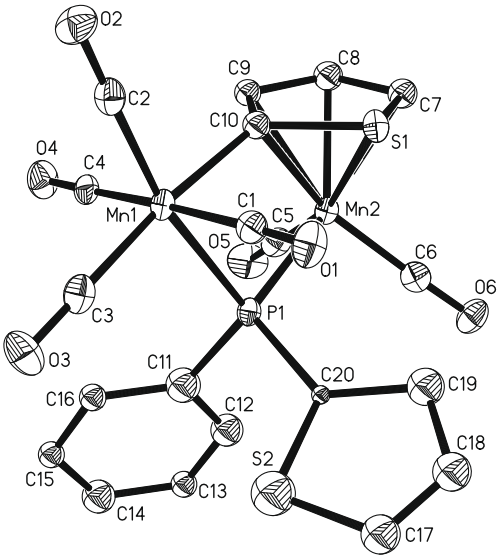

Fig. 4. Molecular structure of [Mn$_2$(CO)$_6$(μ-PPhTh)(μ-η^1,η^5-C$_4$H$_3$S)] (**8**) showing 50% probability thermal ellipsoids. Ring hydrogens are omitted for clarity. Selected bond lengths (Å) and angles (°): Mn(1)–P(1) 2.3711(11), Mn(2)–P(1) 2.2848(11), Mn(2)–S(1) 2.3084(10), Mn(2)–C(7) 2.129(4), Mn(2)–C(8) 2.156(4), Mn(2)–C(9) 2.177(4), Mn(2)–C(10) 2.195(4), Mn(1)–C(10) 2.079(4), C(3)–Mn(1)–C(2) 95.35(17), C(1)–Mn(1)–C(4) 176.33(16), C(3)–Mn(1)–C(10) 171.62(16), C(2)–Mn(1)–C(10) 92.85(16), C(3)–Mn(1)–P(1) 96.13(13), C(2)–Mn(1)–P(1) 168.29(12), C(10)–Mn(1)–P(1) 75.76(10), C(1)–Mn(1)–P(1) 86.82(12), C(1)–Mn(1)–C(10) 92.89(15), C(5)–Mn(2)–P(1) 93.65(13), C(6)–Mn(2)–P(1) 99.04(12), C(5)–Mn(2)–C(6) 88.73(18), C(10)–Mn(2)–P(1) 75.44(10), P(1)–Mn(2)–S(1) 92.31(4), Mn(2)–P(1)–Mn(1) 97.86(4), Mn(1)–C(10)–Mn(2) 110.40(16), C(20)–P(1)–C(11) 101.1(4).

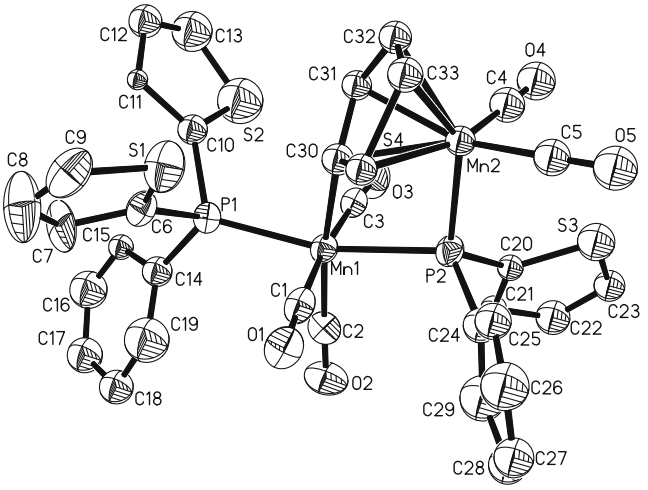

Fig. 5. Molecular structure of $[Mn_2(CO)_5(PPhTh_2)(\mu\text{-}PPhTh)(\mu\text{-}\eta^1,\eta^5\text{-}C_4H_3S)]$ (**9**) showing 50% probability thermal ellipsoids. Ring hydrogens are omitted for clarity. Selected bond lengths (Å) and angles (°): Mn(1)–P(1) 2.2880(15), Mn(1)–P(2) 2.3471(15), Mn(2)–P(2) 2.241(2), Mn(2)–S(4) 2.295(4), Mn(1)–C(30) 2.080(10), Mn(2)–C(30) 2.198(12), Mn(2)–C(31) 2.186(11), Mn(2)–C(32) 2.161(11), Mn(2)–C(33) 2.119(11), C(1)–Mn(1)–C(3) 174.2(2), C(2)–Mn(1)–C(30) 169.5(4), C(2)–Mn(1)–P(1) 97.98(18), C(30)–Mn(1)–P(1) 90.7(4), C(30)–Mn(1)–P(2) 75.9(4), P(1)–Mn(1)–P(2) 165.69(6), C(1)–Mn(1)–P(2) 92.02(16), C(1)–Mn(1)–P(1) 92.03(16), C(1)–Mn(1)–C(30) 86.0(4), C(4)–Mn(2)–C(5) 89.3(7), C(4)–Mn(2)–P(2) 91.6(4), C(5)–Mn(2)–P(2) 97.3(4), P(2)–Mn(2)–S(4) 92.57(10), Mn(2)–P(2)–Mn(1) 98.28(7), Mn(1)–C(30)–Mn(2) 108.4(6), C(24)–P(2)–C(20) 95.8(9).

tion. The structure is related to that of **8** in with a $PPhTh_2$ ligand replacing an equatorial CO group on Mn(1) that lies *trans* to the phosphido bridge. This structure is also very similar to that of $[Mn_2(CO)_5(PTh_3)(\mu\text{-}PTh_2)(\mu\text{-}\eta^1,\eta^5\text{-}C_4H_3S)]$ (**9**) (**P**) (Chart 2) This complex is disordered in the crystal so that the two diastereomers overlap in a 50/50 ratio. In addition the crystal is centric so that there is an exact 50/50 ratio of the enantiomeric forms of each diastereomer. The $^{31}P\text{-}\{^1H\}$ NMR spectrum displays three resonances at δ 51.4, −12.9 and −21.6 in a 2:1:1 ratio. The FAB mass spectrum exhibits the parent molecular ion at *m/z* 798 together with ions due to successive loss of five carbonyl ligands which is consistent with the solid-state structue.

4. Conclusion

In summary, we have demonstrated the reactivity of $PPhTh_2$ towards $[Re_2(CO)_{10-x}(NCMe)_x]$ (x = 0, 1, 2) and $[Mn_2(CO)_{10}]$. Under mild conditions, reactions with the lightly stabilized rhenium complexes give simple substitution products, but carbon–phosphorus bond cleavage is observed under more forcing conditions. Reaction of $[Mn_2(CO)_{10}]$ with $PPhTh_2$ affords three dimanganese complexes of which compounds **8** and **9** have been obtained as a result of carbon–phosphorus bond cleavage and each contains a bridging thienyl ligand bonded to one manganese atom in a η^5-fashion. This observation is similar to that reported for PPh_2Th [25] and PTh_3 [27]. We note that in all instances it is the phosphorus–thienyl bond that is cleaved.

Supplementary material

CCDC 667828, 694818, 667827, 634409 and 634410 contain the supplementary crystallographic data for **3**, **4**, **6**, **8** and **9**, respectively. These data can be obtained free of charge from The Cambridge Crystallographic Data Centre via www.ccdc.cam.ac.uk/data_request/cif.

Acknowledgements

N.B. thanks Sher-e-Bangla Agricultural University for leave to work at Lund University. This research has been sponsored by the Swedish Research Council (VR), the Royal Swedish Academy of Sciences, the Swedish International Development Agency (SIDA) and Ministry of Science and Information & Communication Technology, Government of the People's Republic of Bangladesh.

References

[1] H. Topsøe, B.A. Clausen, F.E. Massoth, Hydrotreating Catalysis, Springer, Berlin, 1996.
[2] J.G. Speight (Ed.), Petroleum Chemistry and Refining, Taylor and Francis, Washington, DC, 1998.
[3] R.J. Angelici, in: R.B. King (Ed.), Encyclopedia of Inorganic Chemistry, vol. 3, Wiley, New York, 1994, pp. 1433–1443.
[4] (a) D.D. Whitehurst, T. Isoda, I. Mochida, Adv. Catal. 42 (1998) 345;
(b) M.J. Ledoux, O. Michaux, G. Agostini, P. Panissod, J. Catal. 102 (1986) 275.
[5] (a) B.C. Gates, J.R. Katzer, G.C.A. Schuit, Chemistry of Catalytic Processes, McGraw-Hill, New York, 1979. pp. 390–447;
(b) G.D. Galpern, in: S. Gronowitz (Ed.), The Chemistry of Heterocyclic Compounds, vol. 44, Part 1, Wiley, New York, 1985, pp. 325–351.
[6] (a) R.A. Sanchez-Delgado, J. Mol. Catal. 86 (1994) 287;
(b) R.J. Angelici, Polyhedron 16 (1997) 3073;
(c) C. Bianchini, A. Meli, J. Chem. Soc., Dalton Trans. (1996) 801.
[7] (a) R.D. Adams, O.-S. Kwon, J.L. Perrin, J. Organomet. Chem. 596 (2000) 102;
(b) R.D. Adams, X. Qu, Organometallics 14 (1995) 2238.
[8] (a) T.A. Pecoraro, R.R. Chianelli, J. Catal. 67 (1981) 430;
(b) R.R. Chianelli, Catal. Rev. 26 (1984) 361;
(c) C. Bianchini, A. Meli, Acc. Chem. Res. 31 (1998) 109;
(d) T.B. Rauchfuss, Prog. Inorg. Chem. 39 (1991) 259;
(e) D.A. Vicic, W.D. Jones, J. Am. Chem. Soc. 121 (1999) 7606.
[9] (a) R.J. Angelici, Acc. Chem. Res. 21 (1988) 387;
(b) N.N. Sauer, R.J. Angelici, J. Catal. 116 (1989) 11;
(c) J.J. Garcia, B.E. Mann, H. Adams, N.A. Bailey, P.M. Maitlis, J. Am. Chem. Soc. 117 (1995) 2179;
(d) R.J. Angelici, Organometallics 20 (2001) 1259. and references therein.
[10] (a) R.J. Angelici, Coord. Chem. Rev. 105 (1990) 61;
(b) R.J. Angelici, Coord. Chem. Rev. 206–207 (2000) 63.
[11] M. Brorson, J.D. King, K. Kiriakidou, F. Prestopino, E. Nordlander, in: P. Braunstein, L.A. Oro, P.R. Raithby (Eds.), Metal Clusters in Chemistry, vol. 2, Wiley-VCH, Weinheim, 1999, pp. 741–781. Chapter 2.6.
[12] (a) R.J. Angelici, Transition Metal Sulphides, NATO ASI Ser 3, vol. 60, 1998, p. 89;
(b) C. Bianchini, A. Meli, Transition Metal Sulphides, NATO ASI Ser. 3, vol. 60, 1998, p. 129;
(c) R.J. Angelici, Bull. Soc. Chim. Belg. 104 (1995) 265.
[13] (a) P.A. Vecchi, A. Ellern, R.J. Anjelici, Organometallics 24 (2005) 2168;
(b) P.A. Vecchi, A. Ellern, R.J. Anjelici, J. Am. Chem. Soc. 125 (2003) 2064.
[14] (a) H. Li, K. Yu, E.J. Watson, K.L. Virkaitis, J.S. D'Acchioli, G.B. Carpenter, D.A. Sweigart, Organometallics 21 (2002) 1262;
(b) A.J. Hernández-Maldonado, R.T. Yang, J. Am. Chem. Soc. 126 (2004) 992.
[15] (a) M.A. Reynolds, I.A. Guzei, R.J. Angelici, J. Am. Chem. Soc. 124 (2002) 1689;
(b) M.A. Reynolds, I.A. Guzei, R.J. Angelici, Organometallics 20 (2001) 1071.
[16] (a) D.G. Churchill, B.M. Bridgewater, G. Parkin, J. Am. Chem. Soc. 122 (2000) 178;
(b) M.S. Palmer, S. Harris, Organometallics 19 (2000) 2114;
(c) J. Torres-Nieto, A. Arévalo, P. García-Gutiérrez, A. Acosta-Ramírez, J.J. García, Organometallics 23 (2004) 4534.
[17] (a) K. Bieger, F. Estevan, P. Lahuerta, J. Lloret, J. Pérez-Prieto, M. Sanaú, N. Siguero, S.-E. Stiriba, Organometallics 22 (2003) 1799;
(b) J. Lloret, F. Estevan, P. Lahuerta, P. Hirva, J. Pérez-Prieto, M. Sanaú, Organometallics 25 (2006) 3156.
[18] A.J. Deeming, S.N. Jayasuriya, A.J. Arce, Y.D. Sanctis, Organometallics 15 (1996) 786.
[19] J.D. King, M. Monari, E. Nordlander, J. Organomet. Chem. 573 (1999) 272.
[20] N.K. Kiriakidou Kazemifar, M.J. Stchedroff, M.A. Mottalib, S. Selva, M. Monari, E. Nordlander, Eur. J. Inorg. Chem. (2006) 2058.
[21] S.P. Tunik, I.G. Koshevoy, A.J. Poë, D.H. Farrar, E. Nordlander, M. Haukka, P.A. Pakkanen, J. Chem. Soc., Dalton Trans. (2003) 2457.
[22] N.K. Kiriakidou Kazemifar, M.J. Stchedroff, M.H. Johannson, M.A. Mottalib, M. Monari, E. Nordlander, Unpublished results.
[23] M.A. Mottalib, S.E. Kabir, D.A. Tocher, A.J. Deeming, E. Nordlander, J. Organomet. Chem. 692 (2007) 5007.
[24] U. Bodensieck, H. Varenkamp, G. Rheinwald, H. Stoeckli-Evans, J. Organomet. Chem. 488 (1995) 85.
[25] A.J. Deeming, M.K. Shinhmar, A.J. Arce, Y.D. Sanctis, J. Chem. Soc., Dalton Trans. (1999) 1153.
[26] M.N. Uddin, N. Begum, M.R. Hassan, G. Hogarth, S.E. Kabir, M.A. Miah, E. Nordlander, D.A. Tocher, J. Chem. Soc., Dalton Trans. (2008) 6219.

[27] M.N. Uddin, M.A. Mottalib, N. Begum, S. Ghosh, A.K. Raha, D.T. Haworth, S.V. Lindeman, T.A. Siddiquee, D.W. Bennett, G. Hogarth, E. Nordlander, S.E. Kabir, Organometallics 28 (2009) 1514.
[28] (a) U. Koelle, J. Organomet. Chem. 155 (1978) 53;
(b) G.W. Harris, J.C.A. Boeyens, N.J. Coville, J. Chem. Soc., Dalton Trans. (1985) 2277;
(c) D.R. Grad, T.L. Brown, J. Am. Chem. Soc. 104 (1982) 6340.
[29] SAINT Software for CCD Diffractometer, V.7.23A, Bruker AXS, 2005.
[30] G.M. Sheldrick, SADBS-2004/1, Program for empirical absorption correction of area-detector data, Institüt für Anorganische Chemie der Universität, Göttingen, Germany, 2005.
[31] Program XS from SHELXTL package, V. 6.12, Bruker AXS, 2001.
[32] Program XL from SHELXTL package, V. 6.10, Bruker AXS, 2001.
[33] M. Khatun, S. Ghosh, D.T. Haworth, S.V. Lindeman, T.A. Siddiquee, D.W. Bennett, G. Hogarth, E. Nordlander, S.E. Kabir, J. Organomet. Chem. 694 (2009) 2941.
[34] S.E. Kabir, F. Ahmed, S. Ghosh, M.R. Hassan, M.S. Islam, A. Sharmin, D.A. Tocher, D.T. Haworth, S.V. Lindeman, T.A. Siddiquee, D.W. Bennet, K.I. Hardcastle, J. Organomet. Chem. 693 (2008) 2657.
[35] U. Flörke, H.J. Haupt, Z. Kristallogr. 201 (1992) 317.